Biophysical Journal, Volume *111*

Supplemental Information

Spontaneous Formation of a Globally Connected Contractile Network in a Microtubule-Motor System

Takayuki Torisawa, Daisuke Taniguchi, Shuji Ishihara, and Kazuhiro Oiwa

Supporting Material

Torisawa et al. Spontaneous formation of a globally connected contractile network in a microtubule-motor system

Supporting Materials and Methods

Measurement of single motor movements

The movements of GFP-fused kinesin proteins were observed using total internal reflection-fluorescence microscopy, as described previously (1). To immobilize fluorescently labeled MTs on a glass surface coated with diphenyldimethoxysilane, 10 μg/mL anti-β-tubulin antibody (sc-58884, Santa Cruz, Dallas, TX) diluted in BRB80 buffer (80 mM PIPES-KOH, 1 mM $MgSO_4$, and 1 mM EGTA) was flowed into the chamber and incubated for 5 min. The chamber was blocked with 1% (w/v) Pluronic F127 dissolved in BRB80 buffer and incubated for 5 min. Following a wash with 0.6–0.7 mg/mL casein (Nacalai) solution, the chamber was filled with ATTO647N-labeled MTs diluted in BRB80 buffer, supplemented with 10 μM taxol and 0.6–0.7 mg/mL casein, and incubated for 5 min. Unbound microtubules were washed away with BRB80 buffer supplemented with 10 μM taxol and 0.6–0.7 mg/mL casein, after which assay buffer (80 mM PIPES-KOH, 2 mM $MgSO_4$, 1 mM EGTA, 2 mM dithiothreitol, 42.5 U/mL glucose oxidase (Sigma), 42.5 U/mL catalase, 25 mM glucose, and 1 mM ATP) containing kinesin molecules was injected. The images were recorded at time intervals of 100 ms, and rolling averages were determined over 4 frames. The positions of motor molecules were determined by 2D Gaussian fitting with custom software (2), and velocities and durations were calculated from each single trace. Velocities were determined by linear fitting to the traces.

Microtubule sliding assay

The sliding movements of crosslinked MTs driven by Eg5 were observed by total internal reflection fluorescence microscopy or confocal laser scanning microscopy (Nikon A1 and Ti-E; Nikon, Tokyo, Japan), using a CFI Plan Apo VC 60X (NA = 0.95, Nikon). To immobilize biotinylated ATTO647N-labeled MTs on the glass chamber coated by Teflon (Furuta, in preparation), 1 mg/mL streptavidin (Wako, Osaka, Japan) in 20 mM PIPES-KOH buffer (pH 6.8) was flowed into the chamber and incubated for 3 min. Then, chamber was blocked with 1% (w/v) Pluronic F127 in BRB80 buffer and incubated for 5 min. Following a wash with 0.6–0.7 mg/mL casein solution, the chamber was filled with ATTO647N-labeled MTs diluted in BRB80 buffer with 10 μM taxol and 0.6–0.7 mg/mL casein, and incubated for 5 min. Eg5 solution (20 nM) in BRB80 buffer with 10 μM taxol was injected into the chamber and incubated for 5 min. The chamber was filled with ATTO565-labeled MTs diluted in BRB80 buffer with 10 μM taxol and 0.6–0.7 mg/mL casein, followed by a 5-min incubation. After washing the chamber with BRB80 buffer containing 10 μM taxol and 0.6–0.7 mg/mL casein, assay buffer was applied to the chamber. The images were recorded at time intervals of 100 ms. Displacement of MTs was traced by manual tracking with custom software (2). The velocity of each MT was determined by a linear fitting to the trajectory.

Supporting Material

Torisawa et al. Spontaneous formation of a globally connected contractile network in a microtubule-motor system

Supporting Figures

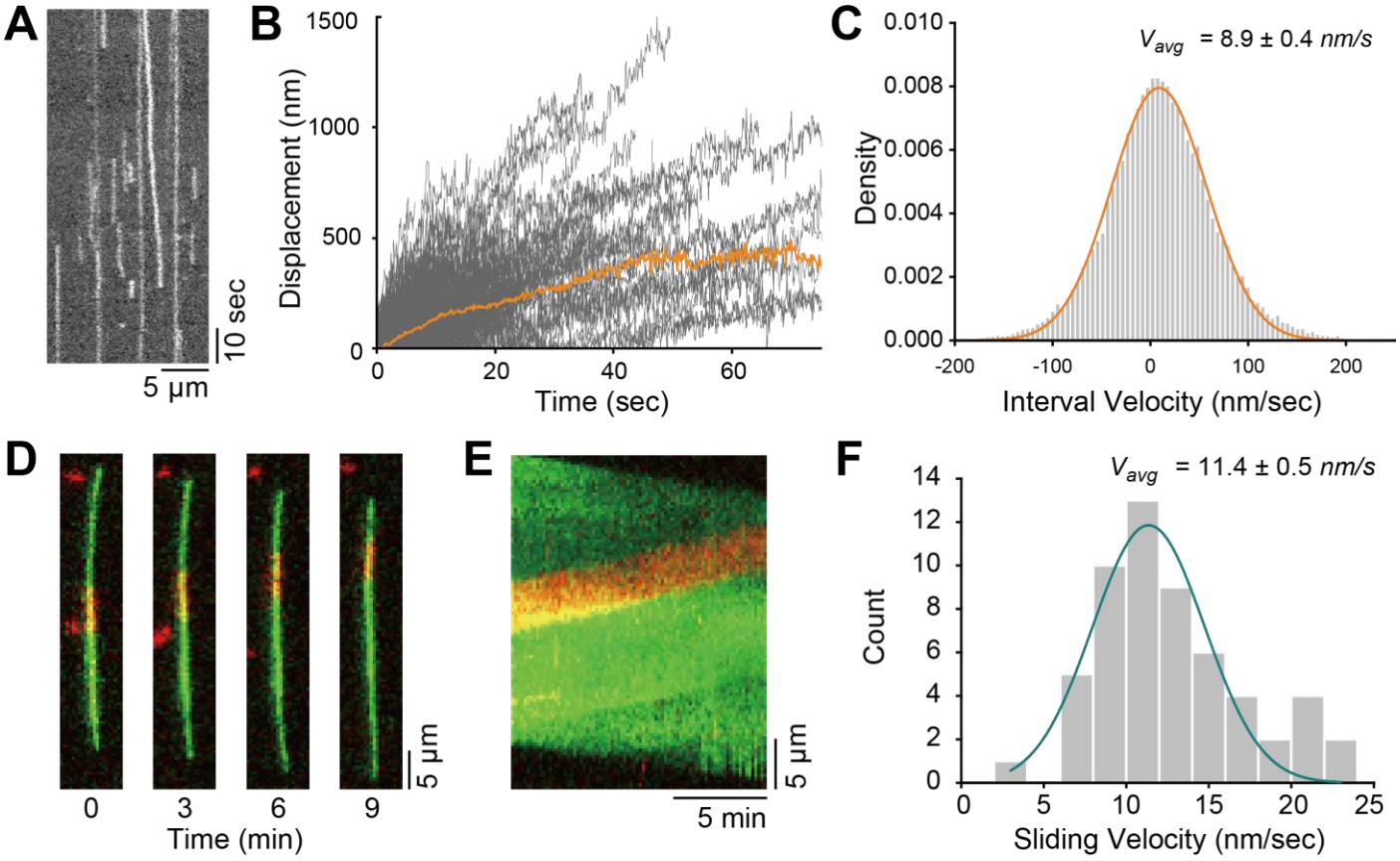

Figure S1. Motile properties of Eg5 used in this study.
(A) Kymograph of GFP-fused Eg5 along a taxol-stabilized GTP-MT in the presence of 1 mM ATP. (B) Trajectories of GFP-fused Eg5 along MTs in the presence of 1 mM ATP (gray lines, n = 239 from 3 experiments). The orange line represents the average trajectory of all traces. (C) Distribution of the interval velocity ($\Delta t = 1.0$ s) obtained from all traces shown in (B). The data were analyzed by Gaussian fitting (orange line, mean = 8.9 ± 0.4 nm/sec). (D) Representative time-lapsed images of MT sliding by Eg5 in the presence of 1 mM ATP. The images of MTs immobilized on glass surface (green) and sliding MTs (red) were merged. The surface MTs were biotinylated and immobilized via biotin-avidin interactions. (E) Kymograph depicting a relative sliding movement between the crosslinked MTs shown in (E). The images of MTs immobilized on a glass surface (green) and sliding MTs (red) were merged. (F) Velocity distribution of MT sliding by Eg5 (n = 56 from 3 experiments). The velocity-distribution data were fitted by Gaussian fitting, and the mean ± SD are shown.

Supporting Material

Torisawa et al. Spontaneous formation of a globally connected contractile network in a microtubule-motor system

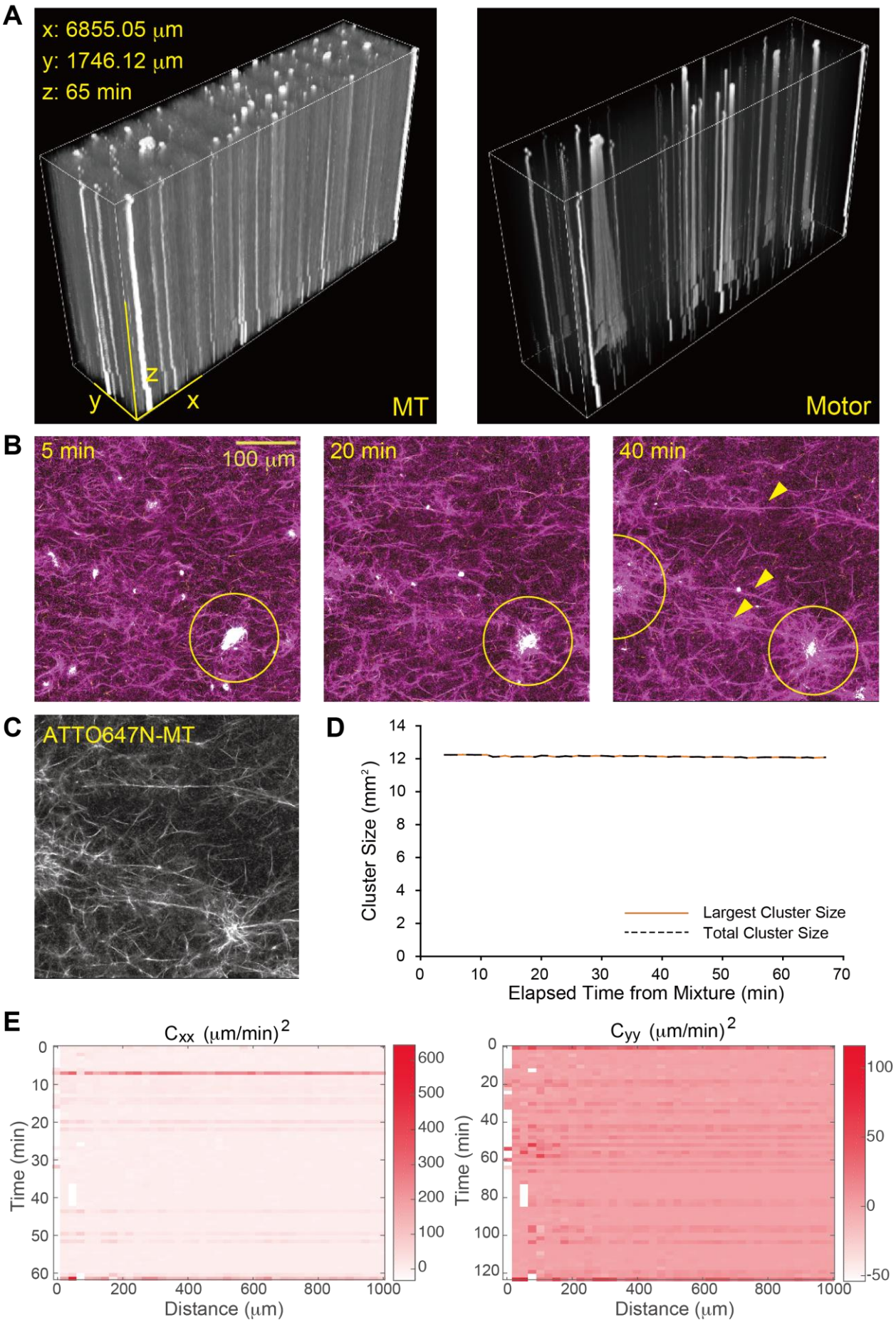

Supporting Material

Torisawa et al. Spontaneous formation of a globally connected contractile network in a microtubule-motor system

Figure S2. Spatiotemporal dynamics of a static network

(A) Three-dimensional representations of the time-dependent evolutionary patterns of MTs and motors in the static network shown in Figure 1C ([Eg5] = 8.91 nM, [tubulin] = 1 μM). (B) Time-series images showing the formation of bundled MT structures under low MT and Eg5 concentrations ([tubulin] = 1 μM, [Eg5] = 4.5 nM). Yellow circles indicate Eg5-accumulated nodes and yellow arrow heads represent MT bundles. The images of ATTO647N-labeled MTs (magenta), ATTO565-labeled MTs (yellow), and GFP-fused Eg5 (cyan) were merged. The times displayed in the images represent the time elapsed following mixing. (C) Image of ATTO647N-labeled MTs shown in (B). (D) Temporal evolution patterns of the total cluster size and the largest cluster. (E) The temporal evolution of the velocity correlation functions in the static network pattern shown in Figure 1. Note that several horizontal stripes appeared in C_{xx} (C_{yy}) are the artifacts created by small drift component in x(y)-direction left even after drift corrections by the software ImageJ. Note also that several blanks appeared within the small distances (< 50μm) are due to shortage of the number of nodes for averaging.

Supporting Material

Torisawa et al. Spontaneous formation of a globally connected contractile network in a microtubule-motor system

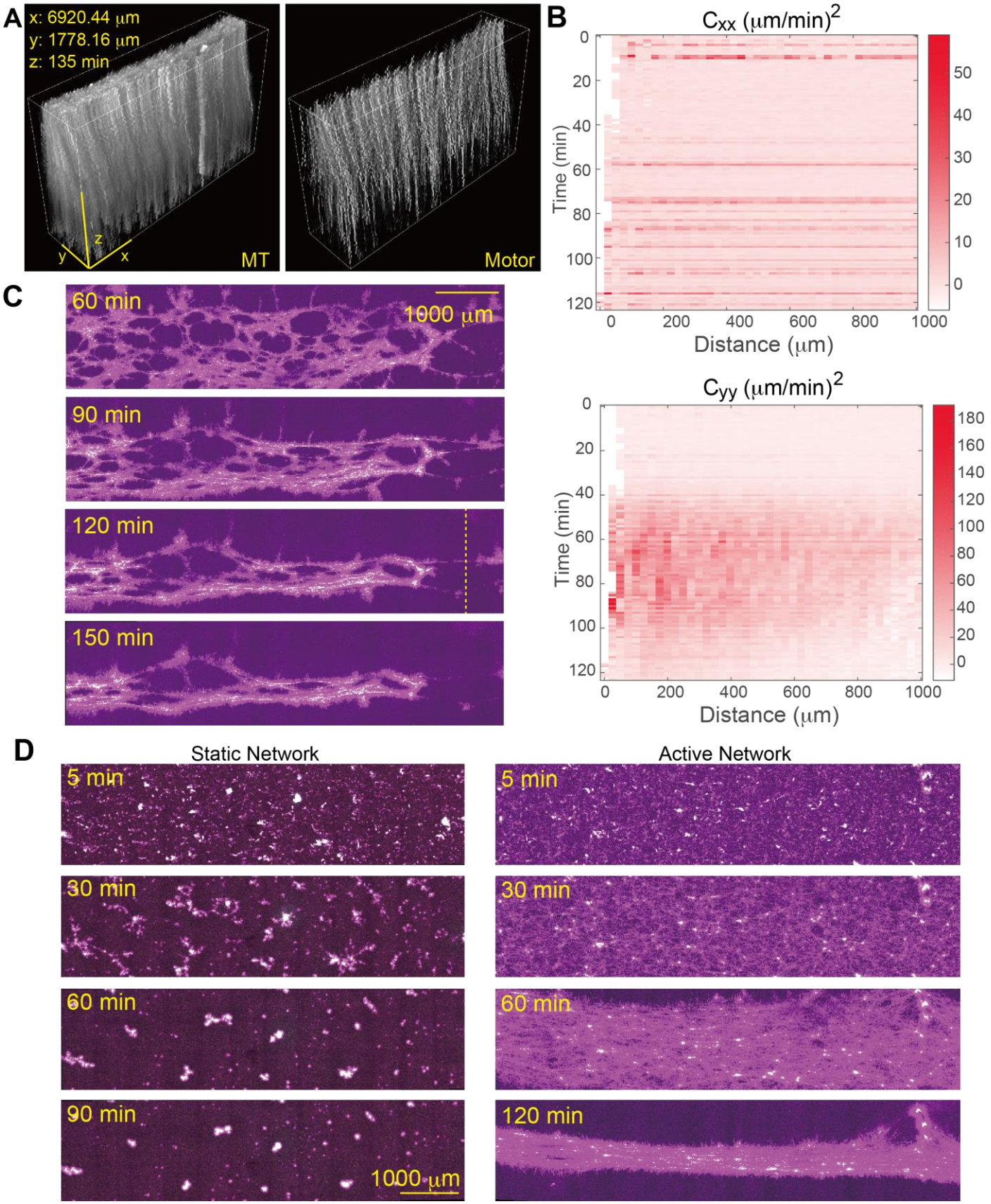

Figure S3. Spatiotemporal dynamics of an active network

(A) Three-dimensional representations of the time-dependent evolutionary patterns of MTs and motors in the active network shown in Figure 2A ([Eg5] = 22.5 nM, [tubulin] = 1 μM). (B) The temporal evolution of the velocity correlation functions in the active network pattern shown in Figure 2. (C) Time-series images

showing occasional self-rupturing of a network ([Eg5] = 22.5 nM and [tubulin] = 1 μM). The images of ATTO647N-labeled MTs (magenta), ATTO565-labeled MTs (yellow), and GFP-fused Eg5 (cyan) were merged. The times displayed in the images represent the time elapsed following mixing. The yellow dashed line indicates the point of rupture. (D) Time-series images showing that different spatiotemporal patterns emerged under the same concentration of Eg5 and MT ([Eg5] = 22.5 nM and [tubulin] = 1 μM). The images of ATTO647N-labeled MTs (magenta), ATTO565-labeled MTs (yellow), and GFP-fused Eg5 (cyan) were merged. The times displayed in the images represent the time elapsed following mixing.

Supporting Material

Torisawa et al. Spontaneous formation of a globally connected contractile network in a microtubule-motor system

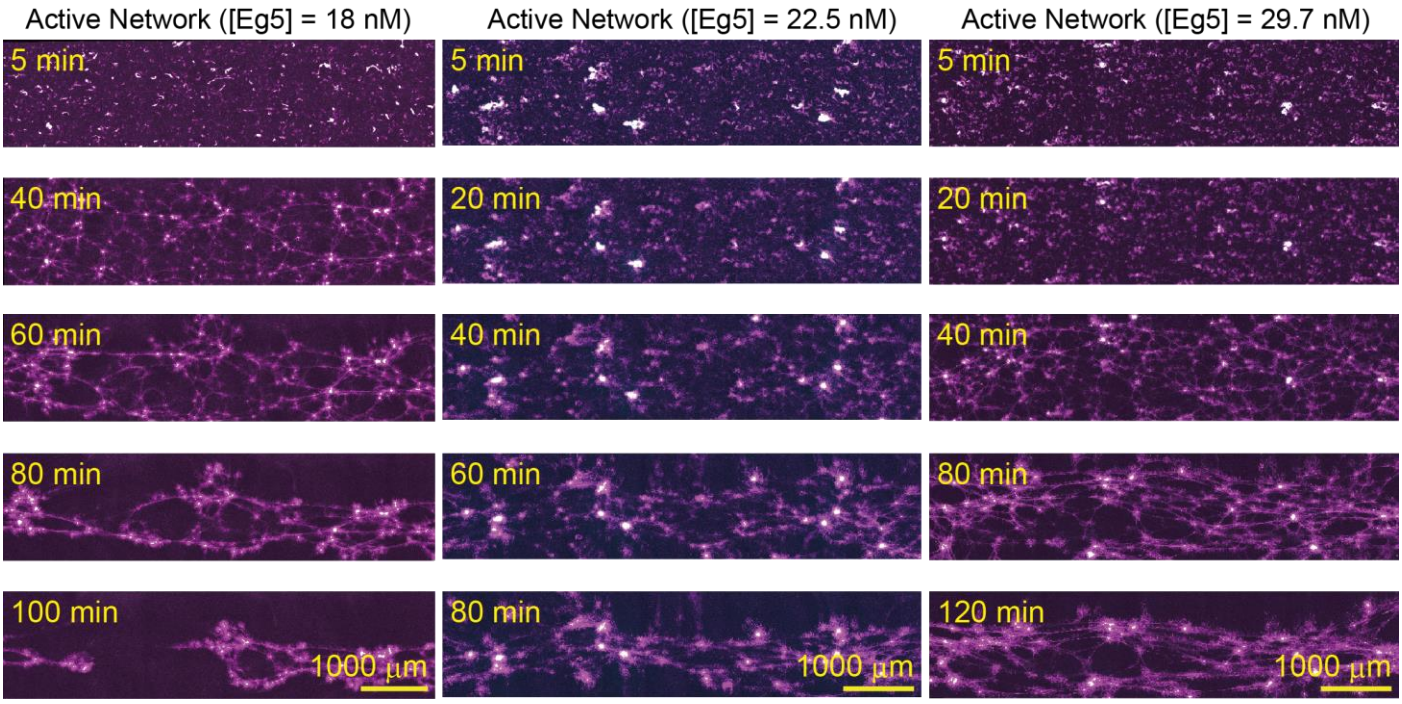

Figure S4. Active networks under various motor concentrations.
Time-series images showing spatiotemporal dynamics of active network under various Eg5 concentrations. The images of ATTO647N-labeled MTs (magenta), ATTO565-labeled MTs (yellow), and GFP-fused Eg5 (cyan) were merged. The times displayed in the images represent the time elapsed following mixing. The temporal evolutionary pattern shown in left displayed a self-rupturing.

Supporting Material

Torisawa et al. Spontaneous formation of a globally connected contractile network in a microtubule-motor system

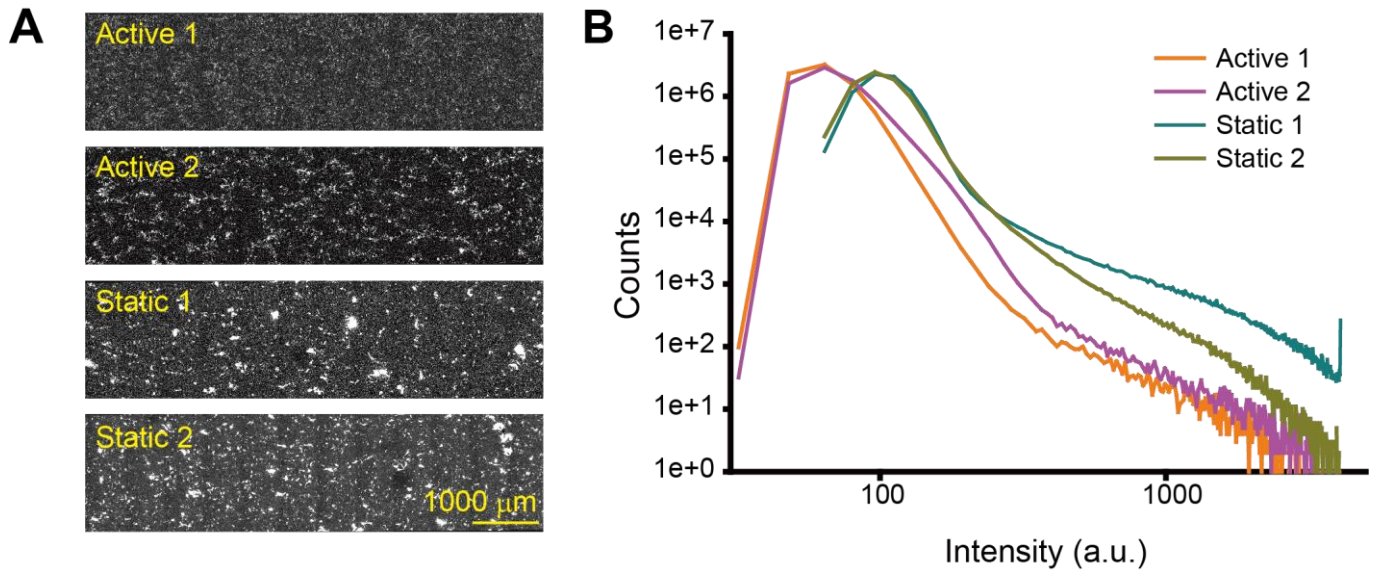

Figure S5. Different spatiotemporal patterns from the same concentration of components

(A) Images of motor channels at the initial dynamics state (5 min following mixing). (B) Distribution of intensities at the early stage of dynamics (5 min).

Supporting Material

Torisawa et al. Spontaneous formation of a globally connected contractile network in a microtubule-motor system

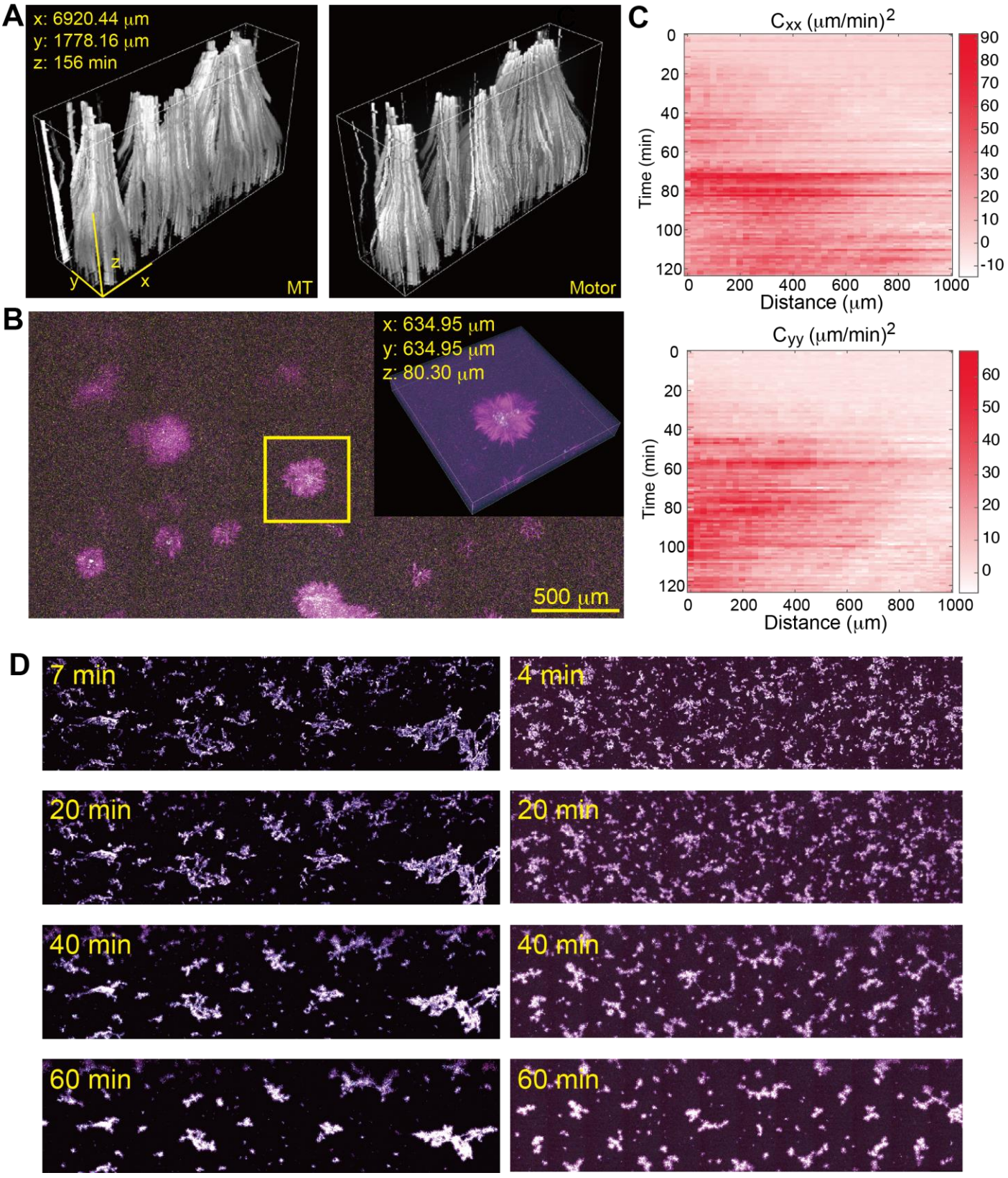

Figure S6. Spatiotemporal dynamics of aggregation

(A) Three-dimensional representations of spatiotemporal dynamics of MTs and motors in the aggregation shown in Figure 3A ([Eg5] = 44.5 nM, [tubulin] = 1 μM). (B) The image showing the formation of astral structures following the rapid contraction of the network ([Eg5] = 44.5 nM, [tubulin] = 1 μM). The images of ATTO647N-labeled MTs (magenta), ATTO565-labeled MTs (yellow), and GFP-fused Eg5 (cyan) were

merged. The inset displays the three-dimensional representation of the astral structure indicated by the yellow square. (C) The temporal evolution of the velocity correlation functions in the aggregation pattern shown in Figure 3. (D) Time-series images showing the examples of temporal evolutionary pattern of aggregation ([Eg5] = 44.5 nM, [tubulin] = 1 μM). The images of ATTO647N-labeled MTs (magenta), ATTO565-labeled MTs (yellow), and GFP-fused Eg5 (cyan) were merged. The times displayed in the images represent the time elapsed following mixing.

Supporting Material

Torisawa et al. Spontaneous formation of a globally connected contractile network in a microtubule-motor system

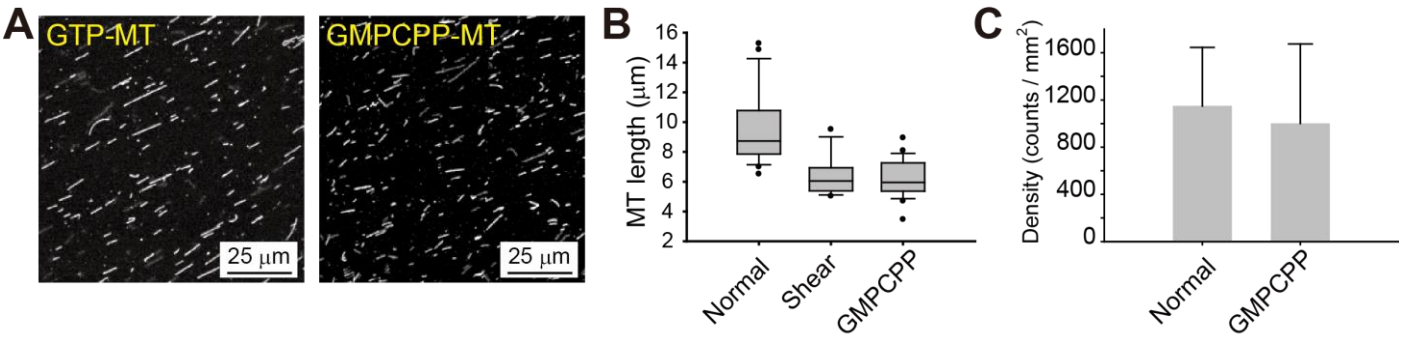

Figure S7. Comparison between GTP- and GMPCPP-MT

(A) Representative images of taxol-stabilized GTP-MTs and GMPCPP-MTs. (B) Box plot of the mean lengths of MTs in assay solution, as measured in self-organization experiments. The mean MT lengths were obtained from 24 (normal; taxol-stabilized GTP-MTs without shear flow), 13 (shear; taxol-stabilized GTP-MTs shortened by shear flow), and 26 (GMPCPP) experiments, respectively. For each experiment, at least 300 MTs were analyzed. The p values from the paired Welch's t-test were found to be 9.775×10^{-6} (normal vs. shear), 9.775×10^{-6} (normal vs. GMPCPP), and 0.7415 (shear vs. GMPCPP), respectively. (C) MT densities in assay solution containing GTP-MTs and GMPCPP-MTs. The p value from the paired Welch's t test was found to be 0.5065.

Supporting Material

Torisawa et al. Spontaneous formation of a globally connected contractile network in a microtubule-motor system

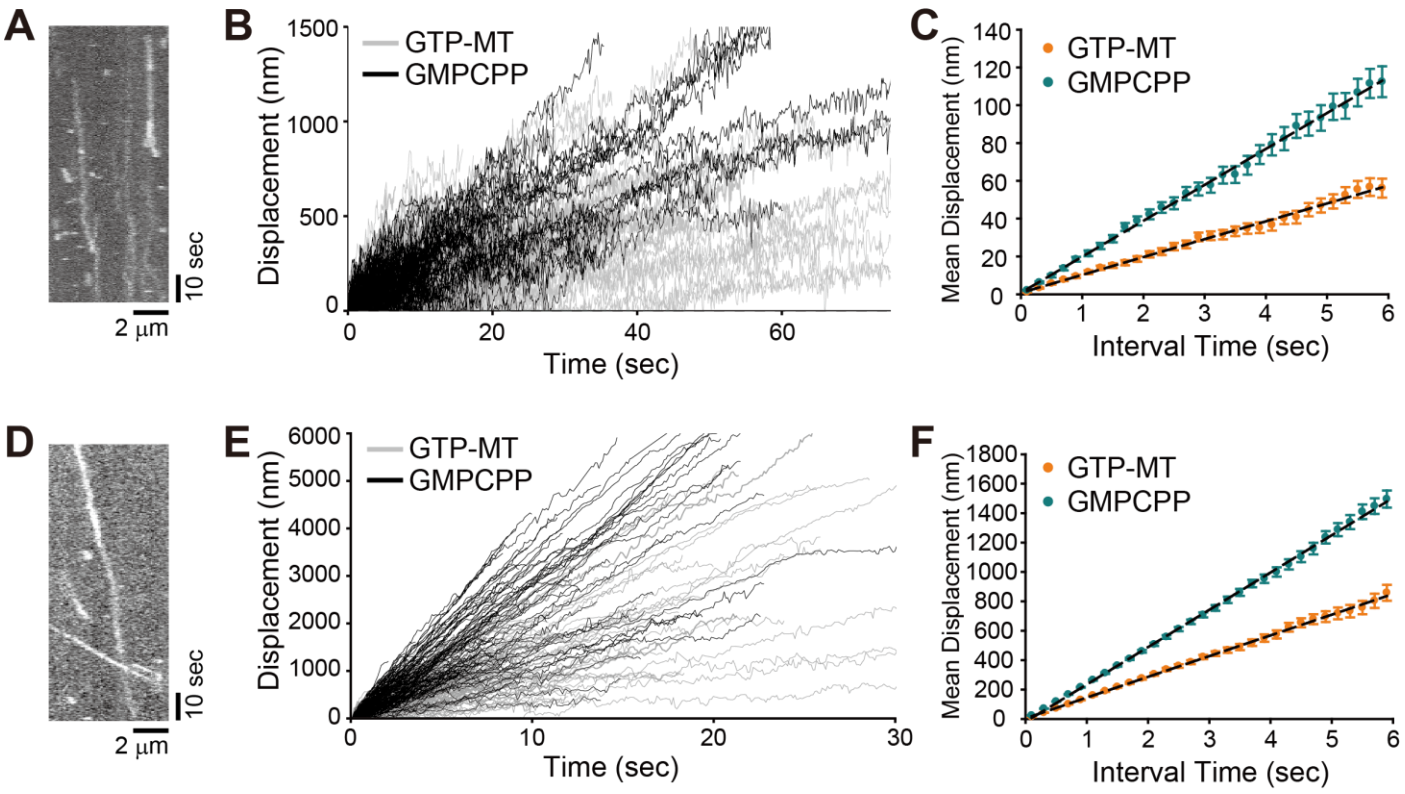

Figure S8. Effects of the motile properties of Eg5 and KIF5B$_{head}$-Eg5$_{tail}$ on GMPCPP-MTs

(A) Kymograph depicting the movements of Eg5 along a GMPCPP-MT in the presence of 1 mM ATP. (B) Trajectories of Eg5 movements on GMPCPP-MTs in the presence of 1 mM ATP. The total trace number was 175 from 3 experiments. (C) Mean displacement plots of Eg5 on taxol-stabilized GTP-MTs and GMPCPP-MTs. The mean velocities obtained from a linear fitting (black line) were 19.0 ± 0.2 nm/s (GMPCPP) and 9.4 ± 0.1 nm/s (GTP), respectively. (D) Kymograph depicting the movements of KIF5B$_{head}$-Eg5$_{tail}$ along a GMPCPP-MT in the presence of 1 mM ATP. (E) Trajectories of KIF5B$_{head}$-Eg5$_{tail}$ movements on GMPCPP-MTs in the presence of 1 mM ATP. The total trace number was 228 from 3 experiments. (F) Mean displacement plots of KIF5B$_{head}$-Eg5$_{tail}$ on taxol-stabilized GTP-MTs and GMPCPP-MTs. The mean velocities obtained from a linear fitting (black line) were 254 ± 1 nm/s (GMPCPP) and 141 ± 1 nm/s (GTP), respectively.

Supporting Material

Torisawa et al. Spontaneous formation of a globally connected contractile network in a microtubule-motor system

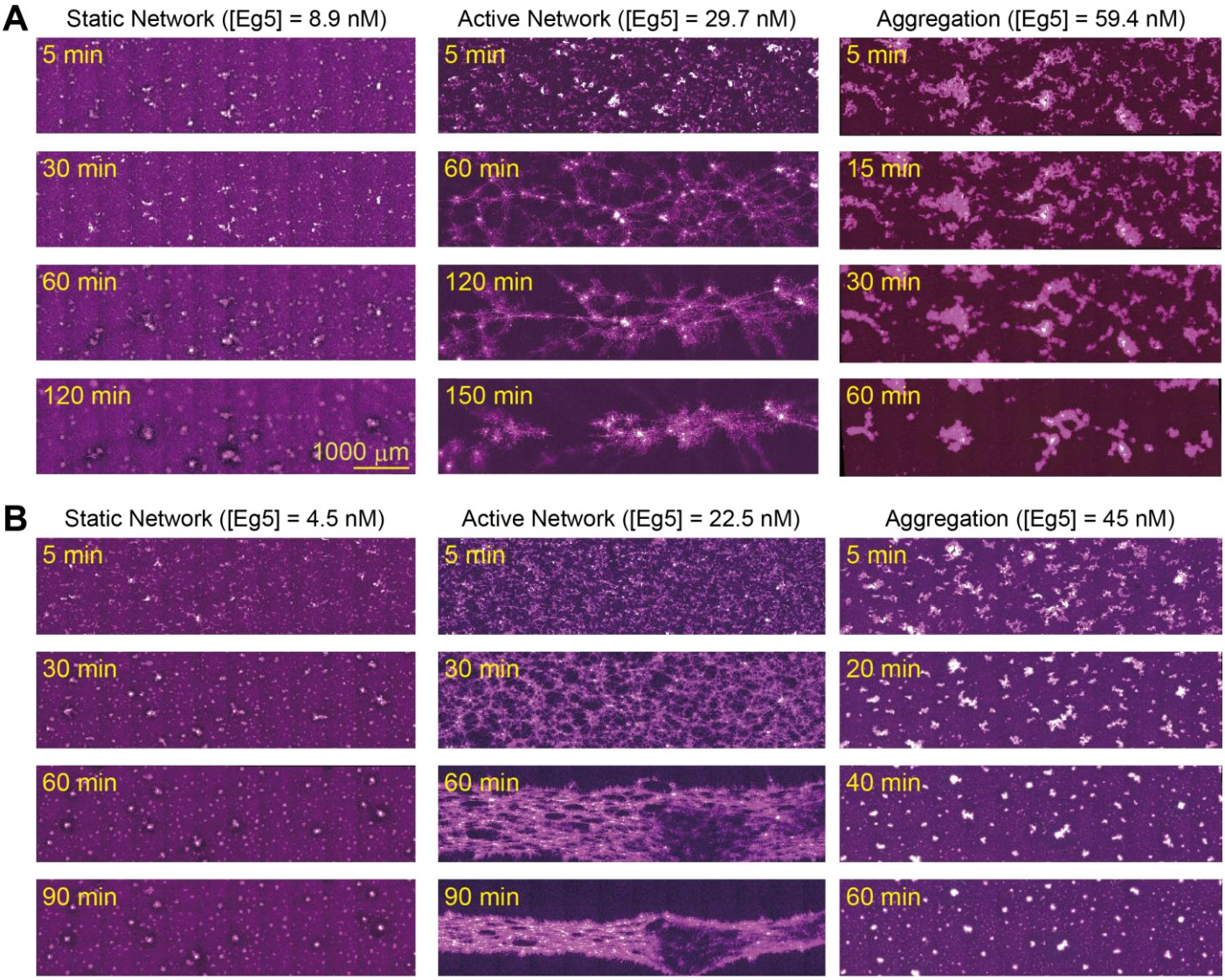

Figure S9. Effects of MT properties on network dynamics

(A) Spatiotemporal dynamics of the Eg5 and GMPCPP-MT system. The images of ATTO647N-labeled MTs (magenta), ATTO565-labeled MTs (yellow), and Eg5 (cyan) are merged. The scale bar (1000 μm) applies to each image shown. The tubulin concentration was 1 μM in all experiments. (B) Spatiotemporal dynamics of the network composed of Eg5 and MTs that were shortened by shear flow. The images of ATTO647N-labeled MTs (magenta), ATTO565-labeled MTs (yellow), and Eg5 (cyan) are merged. The tubulin concentration was 1 μM in all experiments.

Supporting Material

Torisawa et al. Spontaneous formation of a globally connected contractile network in a microtubule-motor system

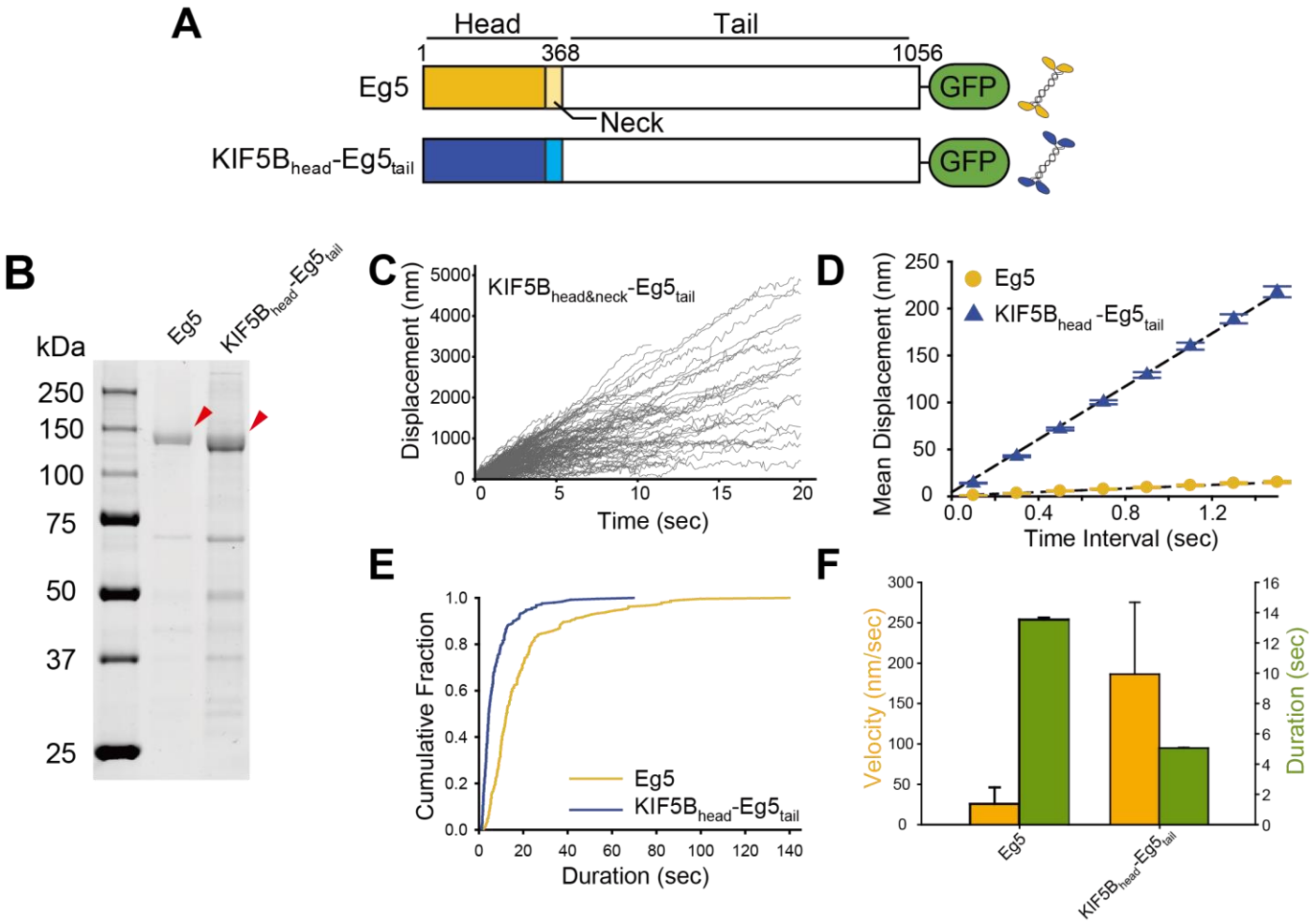

Figure S10. Motile properties of the KIF5B$_{head}$-Eg5$_{tail}$ protein

(**A**) Schematic representations of Eg5 and a chimeric motor, KIF5B$_{head}$-Eg5$_{tail}$. The 6×His and FLAG tag fused to C-terminus of both constructs are not shown. (B) SDS-PAGE image of kinesin constructs. The red arrowheads indicate the purified kinesin constructs. (C) Trajectories of KIF5B$_{head}$-Eg5$_{tail}$ movements along MTs in the presence of 1 mM ATP. The total trace number was 239 from 3 experiments. (D) Mean-displacement plots calculated from the traces of Eg5 (n = 239) and KIF5B$_{head}$-Eg5$_{tail}$ (n = 249). Bars represent the standard error. The dashed lines indicate the linear fit, as determined by the least-squares method. The mean velocities calculated as the slope of fitted lines were 9.4 ± 0.1 nm/s (Eg5, ± SE of fitting) and 141 ± 0.1 nm/s (KIF5B$_{head}$-Eg5$_{tail}$), respectively. (E) Comparison of the durations that Eg5 and KIF5B$_{head}$-Eg5$_{tail}$ were bound to MTs. The cumulative distributions of the durations for Eg5 (black) and KIF5B$_{head}$-Eg5$_{tail}$-GFP (red) are shown. The decay constants derived from a 1-phase exponential decay model were 13.6 ± 0.1 s (± SE of fitting) for Eg5 and 5.1 ± 0.1 s for KIF5B$_{head}$-Eg5$_{tail}$, respectively. (**F**) Double plots of single-molecule velocities and durations of the kinesin constructs. Error bars for the velocities indicate the standard deviations calculated from the raw data, and error bars for the durations represent the standard errors of fitting.

Supporting Material

Torisawa et al. Spontaneous formation of a globally connected contractile network in a microtubule-motor system

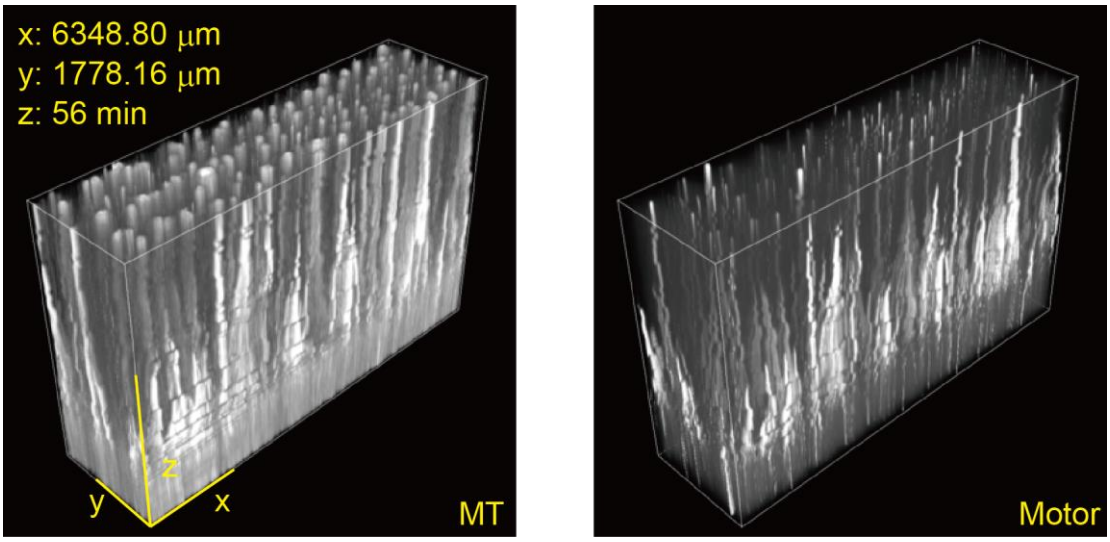

Figure S11. Spatiotemporal dynamics of isolated asters

Three-dimensional representations of the spatiotemporal dynamics of MTs and motors in the isolated asters shown in Figure 4B ([Eg5] = 44.5 nM, [tubulin] = 1 μM)

Supporting Material

Torisawa et al. Spontaneous formation of a globally connected contractile network in a microtubule-motor system

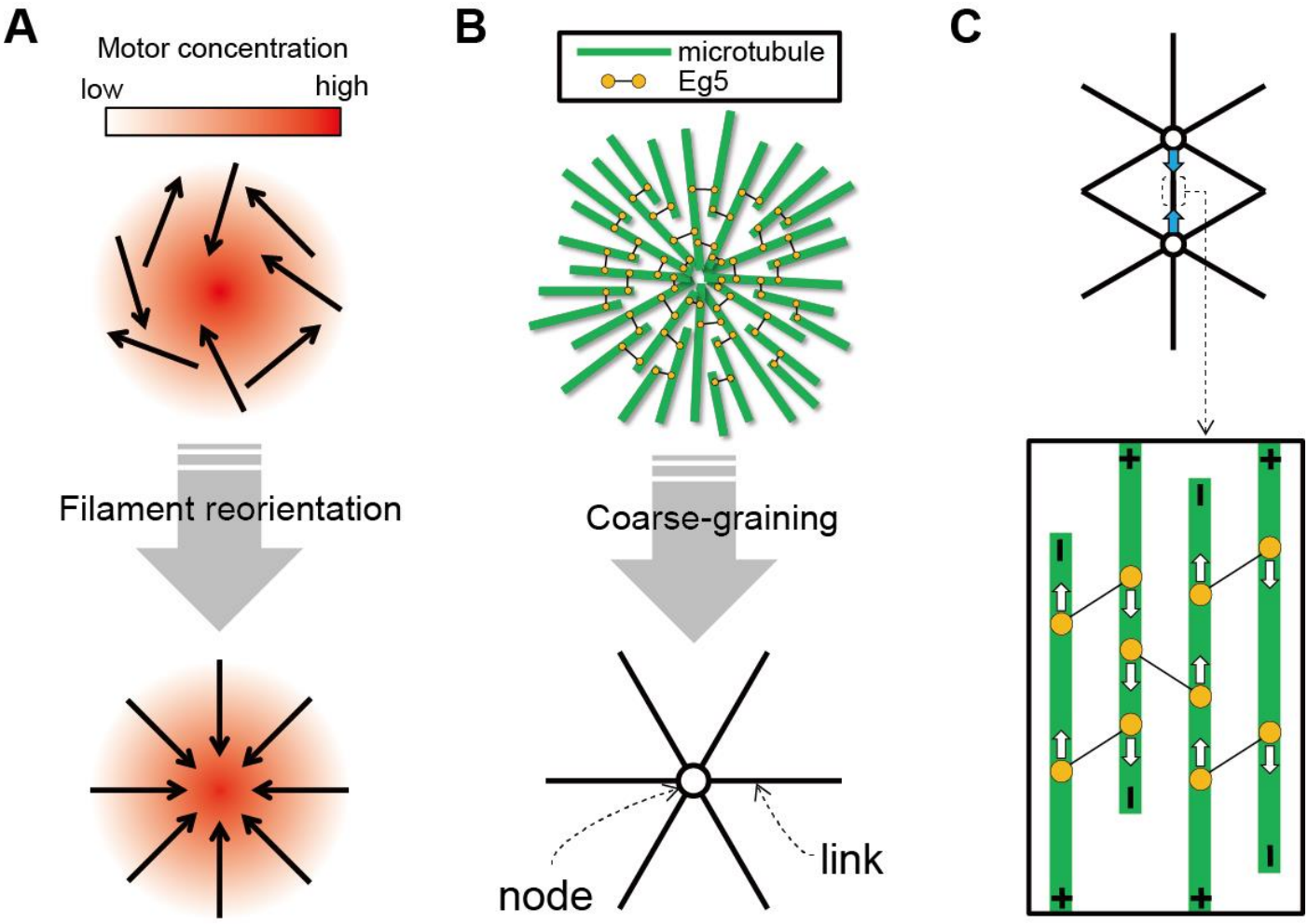

Figure S12. Model schematics

(**A**) Filament reorientation induced by the concentration gradient of motors. Black arrows indicate the local orientations of filaments. Reorientation proceeds as filaments migrate to high-concentration regions to create negative divergence in the local filament orientation, *i.e.* inward pointing asters. (**B**) A single aster-like structure of filament-motor assembly is represented using a node and links. (**C**) The contraction between 2 adjacent nodes originates from the sliding action of the motors. Cyan arrows in the top panel represent the direction of node contraction, whereas white arrows in the bottom panel indicate the direction of filament movement driven by the sliding action of motors. Plus and minus signs represent the filament polarity.

Supporting Material

Torisawa et al. Spontaneous formation of a globally connected contractile network in a microtubule-motor system

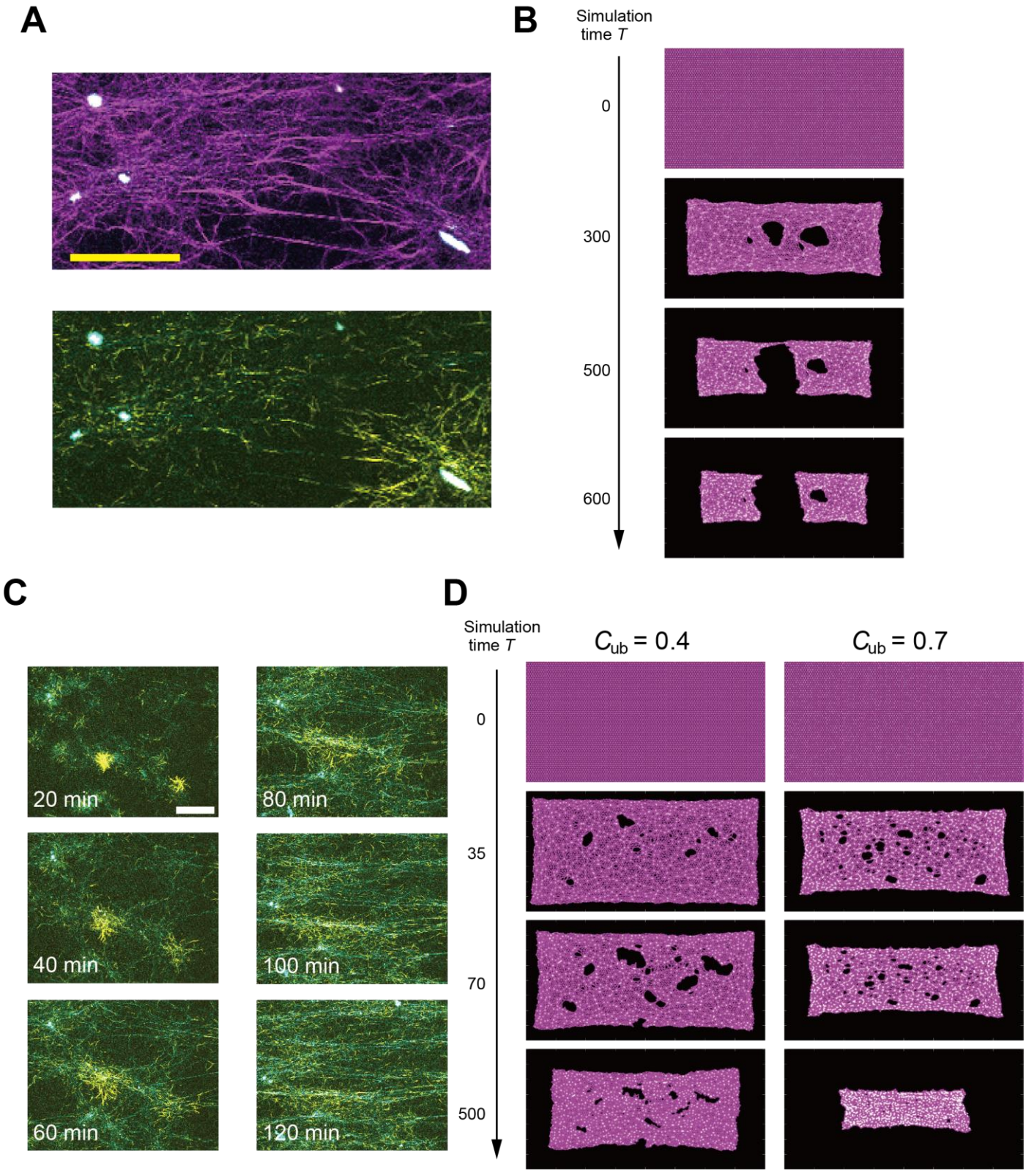

Figure S13. Formation of MT bundles around active nodes and results of a model simulation

(A) MT bundles surrounding active nodes formed 91 min after mixing MTs and Eg5 ([tubulin] = 1 μM, [Eg5] = 22.5 nM). Top: the images of ATTO647N-labeled MTs (magenta) and GFP-fused Eg5 (cyan) were merged. Bottom: the images of ATTO565-labeled MTs (yellow) and GFP-fused Eg5 (cyan) were merged. Bar: 100 μm. (B) Rupture dynamics of an active network. C_{ub} = 0.59, and the other model parameters are the same as those of the active network shown in Figure 5B. (C) MTs were shuttled from their initial location to be

exchanged between active nodes during network formation. *T* is the time measured from the point of mixing MTs and motors ([tubulin] = 1 μM, [Eg5] = 22.5 nM). The images of ATTO565-labeled MTs (yellow) and GFP-fused Eg5 (cyan) were merged. Bar: 100 μm. (D) Simulation result of a modified model, wherein the contraction strength correlates linearly with the motor concentration: $K_{ij} = 0.5(K - k)(C_i + C_j) + k$. $L_{ij} = 0.5(L - l)(C_i + C_j) + l$. The model parameters are the same as those of active network shown in Figure 5B. Left: $C_{ub} = 0.4$. Right: $C_{ub} = 0.7$. Links are depicted by magenta lines and motors are depicted by white circles.

Supporting Material

Torisawa et al. Spontaneous formation of a globally connected contractile network in a microtubule-motor system

Supporting Table

MT	[tubulin] (μM)	[Eg5] (nM)	Max Velocity (nm/sec)	Contractility	Connectivity	Pattern	Observation Time (min, T_f)
GTP	1	4.5	78.3	1.02	1.00	Static	77
GTP	1	8.9	86.7	1.01	1.00	Static	65
GTP	1	14.9 (I)	101.7	1.00	0.99	Active	66
GTP	1	14.9 (II)	126.7	1.55	0.96	Static	88
GTP	1	14.9 (III)	73.3	1.01	1.00	Static	241
GTP	1	14.9 (IV)	80.0	1.20	1.00	Static	107
GTP	1	14.9 (V)	68.3	1.07	1.00	Static	241
GTP	1	19.8 (I)	183.3	1.00	1.00	Active	87
GTP	1	19.8 (II)	193.3	2.05	0.73	Static	167
GTP	1	19.8 (III)	126.7	1.28	1.00	Static	111
GTP	1	22.5 (I)	113.3	2.68	0.99	Active	173
GTP	1	22.5 (II)	145.0	3.87	1.00	Active	301
GTP	1	22.5 (III)	108.3	1.73	1.00	Active	135
GTP	1	22.5 (IV)	145.0	1.50	0.91	Active	78
GTP	1	22.5 (V)	113.3	1.44	1.00	Active	138
GTP	1	22.5 (VI)	258.3	10.77	0.57	Static	101
GTP	1	22.5 (VII)	188.3	6.09	0.05	Static	114
GTP	1	29.7	141.7	1.64	1.00	Active	241
GTP	1	45 (I)	225.0	2.89	0.90	Aggregation	97
GTP	1	45 (II)	98.3	3.08	0.12	Aggregation	147
GTP	1	45 (III)	156.7	2.33	0.50	Static	156
GTP	1	45 (IV)	80.0	3.71	0.06	Aggregation	141
GTP	1	45 (V)	126.7	3.93	0.09	Aggregation	91
GTP	5	45 (I)	-	19.2	0.97	Active	107
GTP	5	45 (II)	-	2.15	0.98	Active	190
GTP	5	45 (III)	51.7	1.54	0.99	Active	241
GTP	5	45 (IV)	-	1.69	0.93	Active	192
GTP	5	45 (V)	43.3	1.13	0.99	Active	241
GMPCPP	1	4.5	93.3	1.02	1.00	Static	85
GMPCPP	1	8.9 (I)	151.7	1.00	1.00	Static	100
GMPCPP	1	8.9 (II)	78.3	1.00	1.00	Static	122
GMPCPP	1	8.9 (III)	63.3	1.07	1.00	Static	241
GMPCPP	1	14.9 (I)	41.7	1.00	1.00	Static	107
GMPCPP	1	14.9 (II)	106.7	1.01	1.00	Static	82
GMPCPP	1	17.8 (I)	125.0	3.94	0.45	Active	308
GMPCPP	1	17.8 (II)	91.7	4.13	0.26	Static	161
GMPCPP	1	19.8 (I)	66.7	1.03	1.00	Static	223
GMPCPP	1	19.8 (II)	178.3	7.35	1.00	Active	241
GMPCPP	1	19.8 (III)	128.3	2.06	0.99	Active	150
GMPCPP	1	22.5 (I)	95.0	2.02	0.81	Active	241
GMPCPP	1	22.5 (II)	61.7	1.00	1.00	Static	241
GMPCPP	1	22.5 (III)	73.3	1.01	1.00	Static	97
GMPCPP	1	22.5 (IV)	158.3	1.03	1.00	Active	114
GMPCPP	1	24.8	83.3	1.18	1.00	Static	132
GMPCPP	1	29.7 (I)	63.3	1.16	1.00	Static	114
GMPCPP	1	29.7 (II)	126.7	2.37	0.87	Active	112
GMPCPP	1	29.7 (III)	115.0	1.54	0.64	Active	301
GMPCPP	1	35.6 (I)	120.0	1.00	0.95	Active	43
GMPCPP	1	35.6 (II)	123.3	2.99	0.97	Active	241
GMPCPP	1	45 (I)	65.0	2.78	0.07	Aggregation	101
GMPCPP	1	45 (II)	105.0	2.77	0.17	Aggregation	76

Supporting Material

Torisawa et al. Spontaneous formation of a globally connected contractile network in a microtubule-motor system

GMPCPP	1	59.4	133.3	2.84	0.26	Aggregation	68
GMPCPP	5	22.5	66.7	1.04	1.00	Static	123
GMPCPP	5	45 (I)	56.7	1.14	0.82	Static	92
GMPCPP	5	45 (II)	46.7	1.34	0.97	Static	118
GMPCPP	5	45 (III)	71.7	1.03	1.00	Static	52
GMPCPP	5	89.1 (I)	58.3	1.09	0.99	Active	83
GMPCPP	5	89.1 (II)	58.3	1.15	0.99	Active	102
GMPCPP	5	89.1 (III)	78.3	1.49	0.96	Active	164
GMPCPP	5	89.1 (IV)	85.0	1.34	1.00	Active	223
GMPCPP	5	118.8	98.3	1.81	0.78	Active	112
GMPCPP	5	148.5 (I)	105.0	2.56	0.58	Active	241
GMPCPP	5	148.5 (II)	65.0	1.48	0.95	Active	301
GMPCPP	5	178.2	-	1.27	1.00	Active	112
Shear	1	4.5	68.3	1.00	1.00	Static	24
Shear	1	14.9	136.7	2.69	0.71	Active	241
Shear	1	19.8	76.7	1.75	0.89	Static	99
Shear	1	22.5 (I)	61.7	1.10	0.99	Static	95
Shear	1	22.5 (II)	98.3	3.09	0.03	Static	98
Shear	1	22.5 (III)	99.5	2.66	0.97	Active	127
Shear	1	45	78.3	2.66	0.03	Aggregation	73
Shear	5	22.5	56.7	1.07	1.00	Static	180
Shear	5	45 (I)	81.7	1.95	0.47	Static	194
Shear	5	45 (II)	60.0	1.15	1.00	Static	126
Shear	5	59.4	70.0	1.64	0.99	Active	301
Shear	5	89.1	100.0	2.06	1.00	Active	178

Table S1. Quantitative analysis of spatiotemporal dynamics of MT-Eg5 network.

MTs used in the experiments, concentrations of tubulin and Eg5, max velocities of active nodes during temporal evolutions, contractility, connectivity, types of patterns, and total observation time are shown. "GTP", "GMPCPP", and "Shear" represent taxol-stabilized MTs without shear flow, GMPCPP-MTs, and GTP-MTs shortened by shear flow, respectively. Max velocity indicates the maximum mean node velocity determined from the temporal evolutionary patterns of mean node velocities. In some experiments with 5 μM of tubulin, the active nodes were too densely distributed to measure velocities.

Supporting Material

Torisawa et al. Spontaneous formation of a globally connected contractile network in a microtubule-motor system

Movie Captions

Movie S1. Spatiotemporal dynamics of a static network

Three dimensional reconstitution of the temporal evolution of the static network shown in Fig. 1C ([Eg5] = 8.9 nM, [tubulin] = 1 μM). The images of ATTO647N-labeled MTs (magenta), ATTO565-labeled MTs (yellow), and GFP-fused Eg5 (cyan) are merged.

Movie S2. Spatiotemporal dynamics of MTs in the static network (1800 × real-time)

The movie displaying the global connectivity of MTs in the static network ([Eg5] = 1.37 nM, [tubulin] = 1 μM). The images of ATTO647N-labeled MTs were shown.

Movie S3. Spatiotemporal dynamics of an active network

Three dimensional reconstitution of the temporal evolution of the active network shown in Fig. 2A ([Eg5] = 22.5 nM, [tubulin] = 1 μM). The images of ATTO647N-labeled MTs (magenta), ATTO565-labeled MTs (yellow), and GFP-fused Eg5 (cyan) are merged.

Movie S4: Temporal evolution pattern of velocity field of the active network

The time-dependent evolutionary pattern of node velocities in the active network shown in Fig. 2A represented by vector fields. The value of velocities are indicated by length of the vectors and colors.

Movie S5: Spatiotemporal dynamics of aggregation

Three dimensional reconstitution of the temporal evolution of the aggregation shown in Fig. 3A ([Eg5] = 45 nM, [tubulin] = 1 μM).The images of ATTO647N-labeled MTs (magenta), ATTO565-labeled MTs (yellow), and GFP-fused Eg5 (cyan) are merged.

Movie S6: Spatiotemporal dynamics of isolated asters

Three dimensional reconstitution of the temporal evolution of the isolated asters shown in Fig. 4B ([$KIF5B_{head}$-$Eg5_{tail}$] = 12.5 nM, [tubulin] = 1 μM). The images of ATTO647N-labeled MTs (magenta), ATTO565-labeled MTs (yellow), and GFP-fused $KIF5B_{head}$-$Eg5_{tail}$ (cyan) are merged.

Movie S7: Spatiotemporal dynamics of MTs in the isolated asters (1800 × real-time)

The movie displaying the lack of global connectivity in the isolated asters ([$KIF5B_{head}$-$Eg5_{tail}$] = 6.25 nM, [tubulin] = 1 μM). The images of ATTO647N-labeled MTs were shown.

Movie S8: Spatiotemporal dynamics of a static network in the coarse-grained model

Model simulation of the static network shown in Fig. 5B. Links are represented in magenta, and motors are represented in white. Model parameters: C_{ub} = 0.1, K = 15, k = 0.5, f = 0.01, L = 0.008, L_c = 0.16, l = 0.08, C_{max} = 1, $\tilde{C}$ = 0.5, ϵ = 0.1, γ = 1, dt = 0.01, N_x = 100, and N_y = 58. The total length of the movie corresponds to 50,000 simulation steps.

Movie S9: Spatiotemporal dynamics of active network in the coarse-grained model

Model simulation of the active network shown in Fig. 5B. Links are represented in magenta, and motors are represented in white. Model parameters: C_{ub} = 0.4, K = 15, k = 0.5, f = 0.01, L = 0.008, L_c = 0.16, l = 0.08, C_{max} = 1, $\tilde{C}$ = 0.5, ϵ = 0.1, γ = 1, dt = 0.01, N_x = 100, and N_y = 58. The total length of the movie corresponds to 50,000 simulation steps.

Movie S10: Spatiotemporal dynamics of aggregation in the coarse-grained model

Model simulation of the aggregation shown in Fig. 5B. Links are represented in magenta, and motors are represented in white. Model parameters: C_{ub} = 0.7, K = 15, k = 0.5, f = 0.01, L = 0.008, L_c = 0.16, l = 0.08, C_{max} = 1, $\tilde{C}$ = 0.5, ϵ = 0.1, γ = 1, dt = 0.01, N_x = 100, and N_y = 58. The total length of the movie corresponds to 50,000 simulation steps.

Supporting Material

Torisawa et al. Spontaneous formation of a globally connected contractile network in a microtubule-motor system

Supporting References

1. Torisawa, T., et al., *Autoinhibition and cooperative activation mechanisms of cytoplasmic dynein.* Nat Cell Biol, 2014. **16**(11): p. 1118-24.
2. Furuta, K. and Y.Y. Toyoshima, *Minus-end-directed motor Ncd exhibits processive movement that is enhanced by microtubule bundling in vitro.* Curr Biol, 2008. **18**(2): p. 152-7.